Structural and Magnetic Properties of $La_{0.9}Sr_{0.1}MnO_3$ Nanoparticles Prepared *via* Sol-gel Process

ALEXANDRU-HORATIU MARINCAS[1], FIRUTA GOGA[1]*, ROXANA DUDRIC[2], CRINA SUCIU[3], ALEXANDRA AVRAM[1], SORIN AUREL DORNEANU[1,4], PETRU ILEA[1,4]*

[1] Babes Bolyai University, Faculty of Chemistry and Chemical Engineering, 11 Arany Janos Str.,400028, Cluj-Napoca, Romania

[2] Babes Bolyai University, Faculty of Physics, 1 Mihail Kogalniceanu Str., 400084, Cluj-Napoca, Romania

[3] CMR Prototech, 38 Fantoftveien Str., Bergen, Norway

[4] Babes Bolyai University, Interdisciplinary Research Institute on Bio-Nano-Sciences, 46 Treboniu Laurian Str., 400271, Cluj-Napoca, Romania

In the present paper, nanosized $La_{0.9}Sr_{0.1}MnO_3$ particles were synthesized via a facile modified sol-gel route using two cheap and environmentally friendly organic chemicals, namely sucrose and pectin. The obtained powders were characterized by thermo gravimetric analysis (TGA), X-ray diffraction (XRD), transmission electron microscopy (TEM), and magnetic measurements. The optimal temperature for obtaining nanosized particles was determined as 1000°C and 1h dwell time was enough to obtain crystalline nanoparticles. Magnetic properties of samples calcined with different calcination period were analyzed and both samples shown a transition temperature around 274 K.

Keywords: $La_{0.9}Sr_{0.1}MnO_3$; sol-gel preparation; thermal analysis; crystal structure; magnetic materials

Lanthanum strontium manganite (LSMO) compounds exhibit great interest due to their colossal magneto-resistance (CMR) and high phase transition temperature (370K), which determine their use in high sensitive magnetic sensors [1, 2]. Other potential applications are fuel cells [3], magnetic refrigeration [4], spintronics [5, 6], and hyperthermia applications [7]. The

$La_{1-x}Sr_xMnO_3$ perovskites exhibit poor oxide ion conductivity (at low temperatures), but despite this, their electronic activity is high enough to be used as cathode materials in SOFC, especially when strontium content is $0.1<x<0.3$ [8, 9].

Several LSMO coatings were developed for thermochromic smart coatings [10] and bamboo-like carbon nanotube (BCNTs) coatings[11]. Recently, manganese perovskite nanoparticles

$La_{1-x}Sr_xMnO_3$ were used to coat $LiMn_2O_4$ lithium-ion battery cathodes, improving $LiMn_2O_4$ cycle capability at high rate, which occurs due to manganese dissolution in electrolytes [12].

Although, the most used method to synthesize LSMO is solid state reaction[13], several alternative routes where developed, including co-precipitation [14], sol-gel [15, 16], solid-state reaction, combustion route [17] and hydrothermal method [18]. Among them, sol-gel processes exhibit several advantages: controlled particle size, uniform distribution of the particles, better dispersion of reactants during synthesis and a good control of stoichiometry[19]. The synthesis route and tempering treatment greatly influence the magnetic and electrical properties of doped manganites[20].

In this paper, $La_{1-x}Sr_xMnO_3$ ($x=0.1$) was synthesized via a modified sol-gel route[21, 22]. The present paper aims to obtain nanosized LSMO at the lowest temperature possible, to investigate the influence of calcination periods on the formation of LSMO, and to determine the magnetic properties of the synthetized nanopowders.

Experimental part

The samples were prepared by the sol-gel method using following reagents: strontium chloride ($SrCl_2 . 6H_2O$, Fluka (99.99%)), manganese acetate ($Mn(CH_3COO)_2 \cdot 4H_2O$, Sigma Aldrich (99.99%)) lanthanum nitrate ($La(NO_3)_2 \cdot 6H_2O$, Alfa Aesar (99.99%)), nitric acid (1M HNO_3, Fluka), and commercially available sucrose and pectin. The reagents were used without any further purification. The sucrose: pectin ratio used for these synthesizes was 5:1.

Stoichiometric amounts of $La(NO_3)_2 \cdot 6H_2O$, $Mn(CH_3COO)_2 \cdot 4H_2O$ and $SrCl_2.6H_2O$ are individually dissolved in hot distilled water and three clear solutions are obtained. The sucrose is dissolved in lanthanum nitrate solution, under vigorous stirring. A homogeneous solution is obtained by mixing together all three solutions under continuous stirring, using a hot plate magnetic stirrer. In order to obtain the gel chain-like network, the *p*H of the solution is maintained acidic by adding nitric acid. During this stage, the pectin is also added and the resulting solution was heated at 70°C and continuously stirred. The clear solution is slowly dried and the gel is slowly formed. The gel aging takes place by continuing the thermal treatment for 2 h. In order to eliminate all the water residues and to prevent gel shrinkage, the obtained gel is slowly dried for another 48 h. Finally, the obtained xerogel sample is calcined in air, at three different temperatures 900, 1000 and 1100°C, respectively, with a dwell time of 2h. The samples are marked as LSMO900, LSMO1000 and LSMO1100, respectively.

Beside this, two more samples from the dried xerogel are calcined at 1000°C, with a heating rate of 5°C/min, followed by two different calcination dwell periods: 1 (LSMO 1h) and 3 hours (LSMO 3h), respectively.

The calcinations processes were carried out using a Kaloria Denkal K8/1100 furnace. The TG-DSC curves were recorded using a TA Instruments DSC SDT Q600 thermogravimetric analyser. Powder diffractograms were recorded, in the 2θ range 20°-90°, using a Bruker D8 Advance AXS X-ray diffractometer. The morphological studies were performed using a JEOL-JEM-1011 electron microscope. Magnetization measurements in the 4.2-300 K temperature range and external magnetic field up to 9T were realized using a 12 T VSM from Cryogenics.

* email: fgoga@chem.ubbcluj.ro; pilea@chem.ubbcluj.ro

Results and discussions

The xerogel TG-DTA curves (fig. 1) exhibit an endothermic process with a slight mass loss (about 5%), up to 153°C. This process is characteristic for the elimination of physical absorbed water. An important exothermic process occurs between 153 and 430°C, with a three-stage mass loss. The 400°C sharp peak is attributed to the decomposition of inorganic precursors and the oxidation of organic compounds, with the release of gases (especially CO_2). The sucrose acts as a fuel and accelerates the decomposition of the inorganic precursors. The TG curves have a flat profile after 430 °C with no mass changes and no peaks are observed on the DTA curve, indicating that no phase transformation occurs.

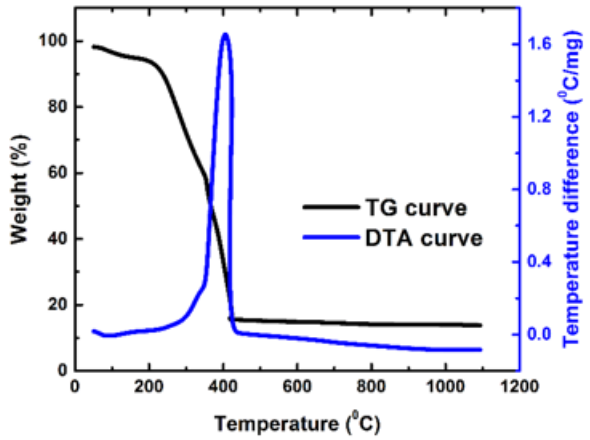

Fig. 1. The TG-DTA curves recorded for xerogel sample

The diffractograms for LSMO900, LSMO1000, and LSMO1100 indicate that single-phase perovskite with rhombohedral structure ($R\bar{3}c$ space group) was obtained at 1000 and 1100°C (fig. 2 ii) and iii)), while in the case of 900°C sample, the temperature was not high enough to lead to a well crystalized perovskite structure (fig. 2 i)).

The broadened XRD maxima indicates that the crystallite is in the nanometer range. The crystallite sizes for LSMO 1h (fig. 3a)) and LSMO 3h (fig. 3b)) were calculated using the Debye-Scherrer formula [23-25]:

$$D_p = \frac{k \cdot \lambda}{\beta_{\frac{1}{2}} \cdot \cos\theta} \quad (1)$$

where β is the peak full width at half maximum (in radians) at the observed peak angle θ, k is the crystallite shape factor (was considered 0.94) and λ=1.540562 Å is the X-ray wavelength.

The average crystallite size was calculated to be about 57 nm with a calcination time of 1h and about 63 nm for the LSMO sample with a 3h calcination period. Nanosized $La_{1-x}Sr_xMnO_3$ (x=0.1) was obtained using both calcination plateaus, but increasing the calcination plateau leads to crystallite growing (table 1).

Table 1
LATTICE PARAMETERS AND CRYSTALLITE SIZES ESTIMATED FROM XRD PATTERNS FOR LSMO CALCINED AT DIFFERENT CALCINATION PERIODS

	a (Å)	c (Å)	D (nm)
LSMO 1h	5.519(8)	13.356(3)	57±1
LSMO 3h	5.519(5)	13.356(3)	63±1

The transmission electron microscopy (TEM) was used to determine the morphology and the particle size of the obtained nanoparticles (fig. 4, fig. 4a) shows small and round non crystalline $La_{0.9}Sr_{0.1}MnO_3$ particles. The particle sizes calculated from the TEM images are about 10-30nm.

For the $La_{0.9}Sr_{0.1}MnO_3$ sample calcined at 1000°C, the microscopy images revealed that the nanoparticles started to agglomerate in clusters, (fig. 4b)). The size of the nanoparticles is between 50-60 nm.

Despite the fact that the higher crystallinity of LSMO can be obtained at the temperature of 1100°C, the aim of the paper was to obtain nanosized $La_{0.9}Sr_{0.1}MnO_3$, and as it can be seen in fig.4c), very large sintered agglomerates were obtained (over 500nm) at 1100°C. Therefore, 1000°C is the recommended temperature for the synthesis of

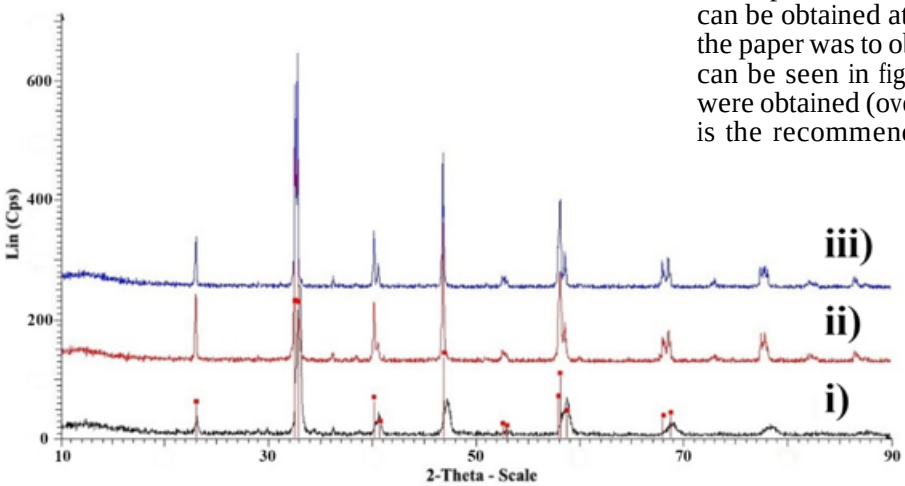

Fig. 2. The XRD patterns for: i) LSMO900, ii) LSMO1000 and iii) LSMO1100

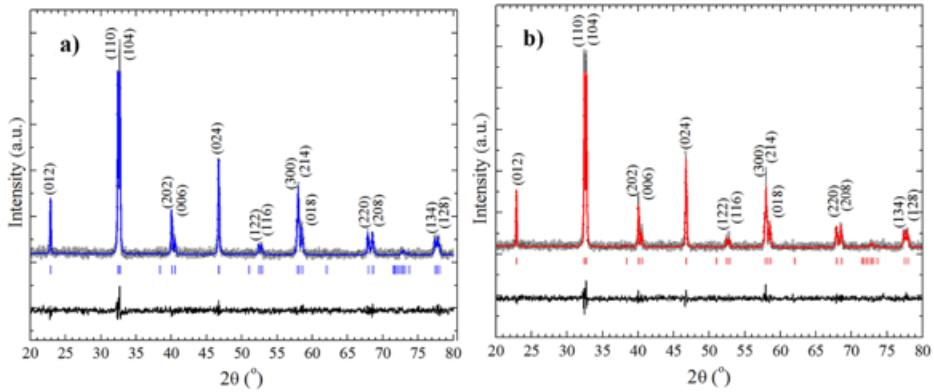

Fig. 3. X-Ray diffraction patterns of LSMO calcined at different calcination durations: a) LSMO1000 1h; b) LSMO1000 3h. Experimental data points are shown as dots, the calculated profile using Rietveld method and difference curve are shown as solid lines.

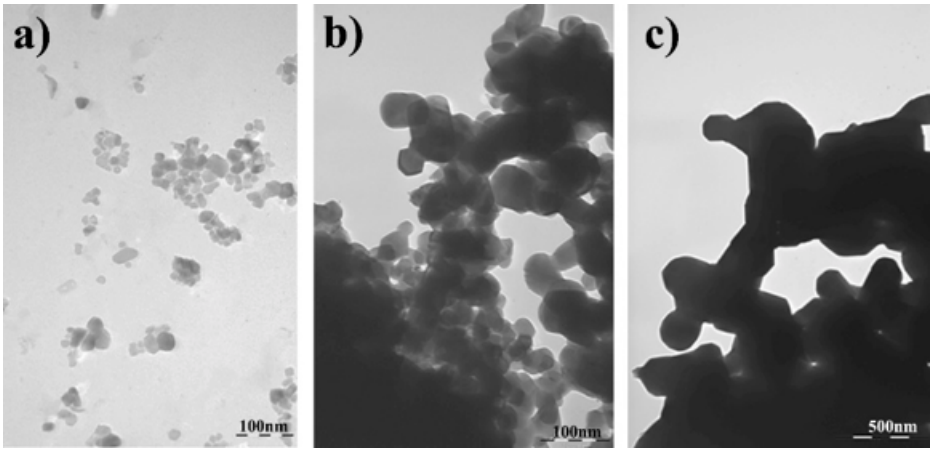

Fig. 4. TEM images for: a) LSMO900, b) LSMO1000 and c) LSMO1100

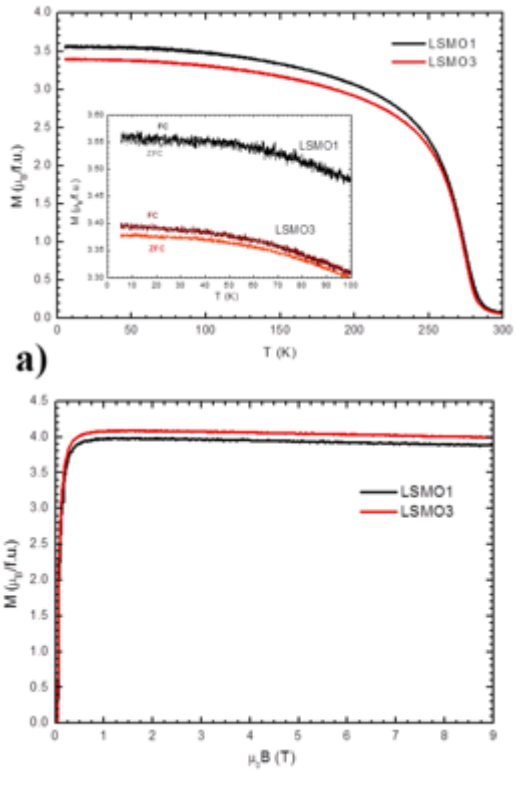

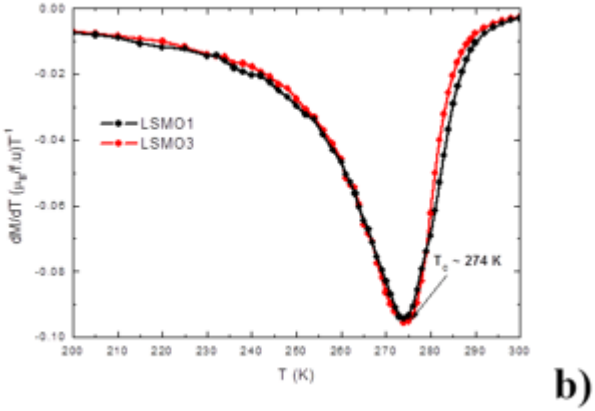

Fig. 5. a) Temperature dependence on field cooled magnetization in 0.2 T of LSMO calcined at different calcination durations. The inset shows the temperature dependence of zero-field cooled and field cooled magnetizations in 0.2 T; b) The transition temperature from paramagnetic to magnetic state; c) Dependence of the applied magnetic field.

nanosized $La_{0.9}Sr_{0.1}MnO_3$ via the proposed modified sol-gel method.

The temperature dependence magnetization after cooling the sample, in external zero magnetic field (ZFC) and in a magnetic field of 0.2 T (FC), was measured under a 2 T magnetic field. fig. 5a) shows the FC magnetization and its variation with the heat treatment duration of the sample. At low temperatures a difference of about 0.2 (μ/f.u.) was noticed between the two samples.

The transition temperature from paramagnetic to magnetic state is obtained as the minimum derivative of the magnetization derivative versus temperature. For both samples, this transition temperature is around 274 K (fig. 5b).

At the temperature of 5K, the magnetization dependence on the applied magnetic field was studied. Magnetization saturation took place in a relative low magnetic field (1T), for both samples (fig. 5c), but the LSMO 3h presented a higher magnetization than LSMO 1h.

Conclusions

Nanosized $La_{0.9}Sr_{0.1}MnO_3$ perovskite was successfully synthesized via the proposed modified sol-gel method. The XRD spectra for the LSMO1000 and LSMO1100 samples showed the presence of a single-phase perovskite with rhombohedral structure (R-3c space group). However, the 900°C temperature was not high enough to lead to a well crystalized perovskite structure. Increasing the calcination plateau, at the 1000°C, from 1h to 3h, leads to an agglomeration of the particles, thus the 1h calcination plateau is enough to obtain LSMO nanoparticles. The TEM revealed that by increasing the calcination temperature of the xerogel to 1000°C, larger nanoparticles (about 65 nm) can be obtained. At 1100°C the nanoparticles sintered in very large clusters. Therefore, the 1000°C temperature is the recommended temperature for obtaining nanosized $La_{0.9}Sr_{0.1}MnO_3$. Magnetic properties of samples calcined with different calcination period were analyzed and both samples shown a transition temperature around 274 K. LSMO 3h had a higher magnetization with the applied magnetic field and both samples (LSMO 1h and LSMO 3h) magnetization saturated in a relative low magnetic field (1T).

Acknowledgements: This research did not receive any specific grant from funding agencies in the public, commercial, or not-for-profit sectors.

References

1. BAAZIZ, H., TOZRI, A., DHAHRI, E., HLIL, E.K., Ceram. Int., **41**, 2015, p. 2955.

2. DAIVAJNA, M.D., RAO, A., OKRAM, G.S., J. Magn. Magn. Mater., **388**, 2015, p. 90.
3. DAI, H., HE, S., CHEN, H., YU, S., GUO, L., J. Power Sources, **280**, 2015, p. 406.
4. ROSTAMNEJADI, A., VENKATESAN, M., KAMELI, P., SALAMATI, H., COEY, J.M.D., J. Magn. Magn. Mater., **323**, 2011, p. 2214.
5. SAHU, D.R., J. Alloys Compd., **503**, 2010, p. 163.
6. MAJUMDAR, S., DIJKEN, S.V., J. Phys. D: Appl. Phys., **47**, 2014, p. 034010.
7. THORAT, N.D., KHOT, V.M., SALUNKHE, A.B., PRASAD, A.I., NINGTHOUJAM, R.S., PAWAR, S.H., J. Phys. D: Appl. Phys., **46**, 2013, p. 105003.
8. RABELO, A.A., MACEDO, M.C.D., MELO, D.M.D.A., PASKOCIMAS, C.A., MARTINELLI, A.E., NASCIMENTO, R.M.D., Materials Research, **14**, 2011, p. 91.
9. YAN, K.-L., FAN, R.-H., CHEN, M., SUN, K., YIN, L.-W., LI, H., PAN, S.-B., YU, M.-X., J. Alloys Compd., **628**, 2015, p. 429.
10. SOLTANI, M., CHAKER, M., JIANG, X.X., NIKANPOUR, D., MARGOT, J., Journal of Vacuum Science & Technology A: Vacuum, Surfaces, and Films, **24**, 2006, p. 1518.
11. BELTRAN-HUARAC, J., CARPENA-NUNEZ, J., BARRIONUEVO, D., MENDOZA, F., KATIYAR, R.S., FONSECA, L.F., WEINER, B.R., MORELL, G., Carbon, **65**, 2013, p. 252.
12. SHI, T., DONG, Y., WANG, C.-M., TAO, F., CHEN, L., J. Power Sources, **273**, 2015, p. 959.
13. FU, Y.-P., Int. J. Hydrogen Energy, **36**, 2011, p. 5574.
14. ZI, Z.F., SUN, Y.P., ZHU, X.B., YANG, Z.R., DAI, J.M., SONG, W.H., J. Magn. Magn. Mater., **321**, 2009, p. 2378.
15. RAVI, S., KARTHIKEYAN, A., Physics Procedia, **54**, 2014, p. 45.
16. ZARBALI, M., GOKTAS, A., MUTLU, I.H., KAZAN, S., SALE, A.G., MIKAILZADE, F., Journal of Superconductivity and Novel Magnetism, **25**, 2011, p. 2767.
17. SHINDE, K.P., THORAT, N.D., PAWAR, S.S., PAWAR, S.H., Mater. Chem. Phys., **134**, 2012, p. 881.
18. MAKOVEC, D., GORSAK, T., ZUPAN, K., LISJAK, D., J. Cryst. Growth, **375**, 2013, p. 78.
19. REN, Q., ZHANG, Y., CHEN, Y., WANG, G., DONG, X., TANG, X., J. Sol-Gel Sci. Technol., **67**, 2013, p. 170.
20. SHINDE, K.P., PAWAR, S.S., PAWAR, S.H., Appl. Surf. Sci., **257**, 2011, p. 9996.
21. TIKKANEN, H., SUCIU, C., WERNHUS, I., HOFFMANN, A.C., Ceram. Int., **37**, 2011, p. 2869.
22. SUCIU, C., GAGEA, L., HOFFMANN, A.C., MOCEAN, M., Chem. Eng. Sci., **61**, 2006, p. 7831.
23. LANGFORD, J.I., WILSON, A.J.C., J. Appl. Crystallogr., **11**, 1978, p. 102.
24. IBANESCU, M., MUSAT, V., TEXTOR, T., MAHLTIG, B., Rev. Chim. (Bucharest), **65**, no. 6, 2014, p. 689.
25. PICA, A., FICAI, D., GURAN, C., Rev. Chim. (Bucharest), **63**, no. 5, 2012, p. 459.

Manuscript received: 9.07.2018